



Synthesis, crystal structures and photophysical properties of novel boron-containing derivatives of phenalene with bright solid-state luminescence



Weibo Yan^{a,b}, Chenming Hong^a, Guankui Long^b, Yang Yang^b, Zhiwei Liu^a,
Zuqiang Bian^{a,*}, Yongsheng Chen^b, Chunhui Huang^a

^a State Key Laboratory of Rare Earth Materials Chemistry and Applications, Peking University, Beijing 100871, PR China

^b State Key Laboratory for Functional Polymer Materials and Center for Nanoscale Science & Technology, Institute of Polymer Chemistry, College of Chemistry, Nankai University, Tianjin 300071, PR China

ARTICLE INFO

Article history:

Received 6 November 2013

Received in revised form

23 February 2014

Accepted 10 March 2014

Available online 20 March 2014

Keywords:

Aggregation induced emission

Intramolecular effect

Organoboron compound

Phenalene

Push–pull chromophore

Solid-state fluorescence

ABSTRACT

A novel series of boron-containing derivatives of phenalene have been synthesized. These compounds with emission changes from green, yellow to red were obtained by introducing electron-donating or electron-withdrawing substituent groups. Electron density distribution and energy levels of new compounds were calculated by density functional theory. The results show that the HOMO orbitals are delocalized over the whole molecule of the π -conjugated framework, with the LUMO orbitals mainly delocalized over the phenalene plane. The single-crystal structure demonstrates that the bulky substituents prevent the fluorophores forming short intermolecular interactions, which helps to avoid energy loss via non-irradiative decay and benefits enhancing the solid-state fluorescence emission of the compounds. Moreover, keeping intramolecular push–pull electronic structure was found to be also in favor of strengthening the fluorescent intensity of this kind of compounds.

© 2014 Elsevier Ltd. All rights reserved.

1. Introduction

In recent years, organoboron compounds with high efficient fluorescence in solution or solid state have attracted considerable attention because of their excellent photophysical properties and potential use in molecular sensors [1], biomolecular probes [2] and especially in the construction of optoelectronic devices such as organic light emitting devices (OLEDs) [3]. Many new organoboron compounds, oligomers and polymers with strong fluorescence have been synthesized, which show big potential for applications such as OLEDs, etc. [4].

Recently, solid-emissive fluorescent compounds based on silole have been much studied by Prof. Tang's group. These molecules with strong solid emission based on an aggregation-induced emission (AIE) concept, have shown good performance on molecular sensors and OLEDs [5]. Whilst some peculiar boron-based fluorophores with strong emission properties have been also explored and showed good applications in OLEDs [6]. So it is very meaningful to develop new boron-containing compounds with AIE

property, aiming at getting the strong solid-emissive fluorescent boron compounds. The fluorescent boron-containing compounds family can mainly be divided into two classes: 1) three-coordinate boron compounds and 2) four-coordinate boron compounds [7]. Three-coordinate boron is generally electron withdrawing and its vacant p orbital allows for conjugation of organic π systems with and through boron. But its vacant p also leads to kinetic instability towards air and moisture; so many stable three-coordinate boron compounds require steric hindrance of the p orbital by bulky substituents. Four-coordinate boron compounds with the form BR_3X are tetrahedral and generally contain a bidentate quinolato ligand [7]. In these compounds, p orbital has been used to coordinate, which leads to greater stability towards air and water than three-coordinate boron compounds.

We have reported a new series of four-coordinate boron compounds: 2,2-difluoro-3-R-2-bora-s-3-aza-1-oxophenalene (DFBPLY), boron–fluorine complexes with a large planar π -conjugated chromophore and phenalene dye as core in our past research work [8]. These DFBPLY compounds have AIE property and show emission of moderate intensity in the solid state. In this report, by introducing steric bulk and groups bearing the different π -electronic effects to the different sites on the phenalene dye (Fig. 1), we further

* Corresponding author.

E-mail address: bianzq@pku.edu.cn (Z. Bian).

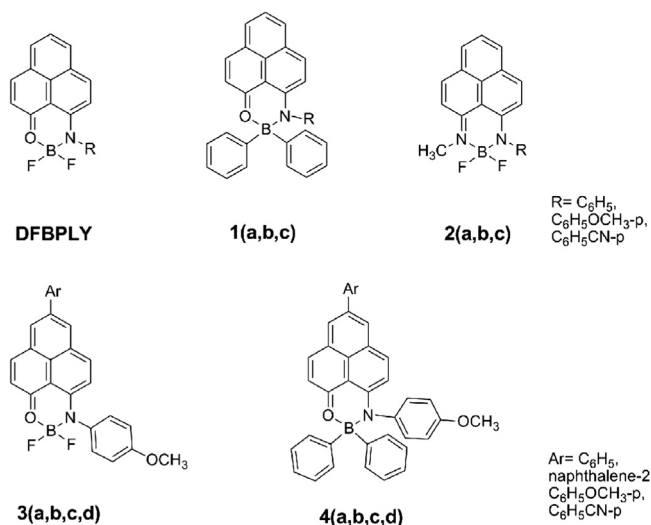


Fig. 1. Molecular structures of DFBPLY and phenalene-based boron complexes: **1**, **2**, **3**, **4**.

study the effect caused by different substitutes on the compound's fluorescent emission on the basis of previous compounds. These new four-coordinate boron compounds can be considered to contain a phenalene-bidentate ligand and they are very stable in the air and not sensitive to humidity.

2. Experimental section

2.1. Materials and methods

Bromobenzene, 2-bromonaphthalene, 1-bromo-4-methoxybenzene and 4-bromobenzonitrile were bought from Alfa Aesar Company. All solvents were purified by standard methods prior to use. The procedure for synthesis of compounds **A1**–**A13** was shown in [Supporting information](#). The ¹H NMR and ¹³C NMR spectra were measured on a Bruker AC-300 and a Bruker AC-400 using tetramethylsilane (TMS) as internal standard. HRMS were recorded on a Fourier transformed ion cyclotron resonance mass spectrometer (Bruker, APEX IV FTMS) with an ESI resource. Absorption spectra were observed with a JASCO V-570 spectrophotometer and fluorescence spectra were measured with a Fluora Max-3P spectra photometer. The absolute PL quantum yields of solid films were measured in a Nanolog Fluorolog-3-2-IHR320 combined measurement system by a F-3018 integrating sphere. A Bruker SMART 1000 CCD automatic diffractometer was used for data collection at 113(2) K using graphite monochromated MoK α -radiation ($\lambda = 0.71073$ Å). Cyclic voltammetry was performed with a computer controlled CHI600C electrochemical workstation using a conventional three electrode configuration consisting of a one compartment electrolysis cell with a platinum button as a working electrode, platinum wire as a counter electrode, and Ag/AgCl reference electrode. Cyclic voltammograms were obtained in dichloromethane (1×10^{-3} M) using tetrabutylammonium hexafluorophosphate (TBAPF₆) (0.1 M) as the supporting electrolyte at scan rate of 0.1 V s⁻¹. Fc/Fc⁺ was used as internal reference during the measurement.

2.2. Synthesis

2.2.1. Synthesis of compound **1a**

To a degassed solution of **A4** [8] (0.1 g, 0.31 mmol) in dry THF, fresh PhMgBr solution was added {Grignard reagent PhMgBr was prepared from PhBr (1.0 mmol) and Mg (2.0 mmol) refluxed in THF

(10 mL)}, the resulting mixture was stirred at ambient temperature for 2 h under an Ar atmosphere. The color of the solution turned from yellow to pink. TLC indicated that the starting material had completely reacted. Then excess solvent was removed under reduced pressure and the crude product was purified by column chromatography (silica gel, petroleum ether/ethyl acetate = 10:1, v/v) to give **1a** (0.08 g, 0.18 mmol) as a jujube red powder, yield: 58.1%. ¹H NMR (300 MHz, CDCl₃): δ [ppm] = 8.02 (1H, d, $J = 9.0$ Hz), 7.92 (1H, d, $J = 7.8$ Hz), 7.79 (1H, d, $J = 7.2$ Hz), 7.49–7.44 (5H, m), 7.24 (2H, d, $J = 8.1$ Hz), 7.18–7.11 (9H, m), 6.96–6.93 (2H, m), 6.76 (1H, d, $J = 9.6$ Hz). ¹³C NMR (400 MHz, CDCl₃): δ [ppm] = 168.34, 158.56, 142.82, 141.15, 139.88, 133.39, 132.53, 128.90, 127.52, 126.90, 126.78, 126.66, 126.00, 125.69, 125.62, 123.85, 123.28, 119.62, 109.91. HRMS (ESI) calcd. for [C₃₁H₂₂ONB + H]⁺: 436.18726; found: 436.18608.

2.2.2. Synthesis of compound **1b**

Synthesis of the compound **1b** is according to the method of synthesis of compound **1a**.

Yield: 40.9%. ¹H NMR (300 MHz, CDCl₃): δ [ppm] = 8.01 (1H, d, $J = 9.3$ Hz), 7.90 (1H, d, $J = 7.8$ Hz), 7.77 (1H, d, $J = 7.5$ Hz), 7.48–7.45 (5H, m), 7.19–7.12 (7H, m), 6.84 (2H, d, $J = 9.0$ Hz), 6.74 (1H, d, $J = 9.6$ Hz), 6.68 (1H, d, $J = 9.0$ Hz), 3.77 (3H, s). ¹³C NMR (400 MHz, CDCl₃): δ [ppm] = 168.10, 158.83, 158.19, 141.03, 139.74, 135.78, 133.81, 133.31, 132.44, 128.54, 126.83, 126.05, 125.87, 125.68, 123.84, 123.24, 119.71, 114.07, 109.89, 55.35. HRMS (ESI) calcd. for [C₃₂H₂₄O₂NB + H]⁺: 466.19784; found: 466.19927.

2.2.3. Synthesis of compound **1c**

Synthesis of the compound **1c** is according to the method of synthesis of compound **1a**.

Yield: 34.8%. ¹H NMR (300 MHz, CDCl₃): δ [ppm] = 8.07 (1H, d, $J = 9.6$ Hz), 7.89 (1H, d, $J = 7.2$ Hz), 7.87 (1H, d, $J = 7.2$ Hz), 7.81 (1H, d, $J = 9.6$ Hz), 7.52 (1H, t, $J = 7.5$ Hz), 7.47–7.42 (6H, m), 7.33–7.31 (1H, m), 7.25 (1H, d, $J = 9.0$ Hz), 7.18–7.10 (8H, m). ¹³C NMR (400 MHz, CDCl₃): δ [ppm] = 169.53, 158.53, 147.32, 142.22, 141.05, 134.27, 133.76, 133.42, 128.69, 128.19, 126.97, 126.61, 126.44, 125.94, 125.85, 125.58, 124.34, 123.43, 118.94, 118.36, 110.46, 110.27. HRMS (ESI) calcd. for [C₃₂H₂₂ON₂B + H]⁺: 461.18252; found: 461.18206.

2.2.4. Synthesis of compound **2a**

To the solution of **A7** (0.120 g, 0.42 mmol) in *o*-xylene (30 mL), BF₃·Et₂O (1 M) (0.5 mL, 0.5 mmol) was added. The yellow solid precipitated immediately from the solution. Then the mixture was stirred at 130 °C for 16 h until the starting material completely disappeared on the TLC plane. After the mixture was cooled down, saturated aqueous NaHCO₃ was added to remove excess BF₃ and HF. The mixture was then extracted by CH₂Cl₂ and the obtained organic phase was dried by Na₂SO₄, filtrated and concentrated to obtain the crude product, which was purified by column chromatography (silica gel, petroleum ether/ethyl acetate = 1:1, v/v) to give **2a** (0.074 g, 0.22 mmol) as a bright red powder, yield: 53.1%. ¹H NMR (300 MHz, CDCl₃): δ [ppm] = 8.21 (1H, d, $J = 9.6$ Hz), 8.00 (1H, d, $J = 7.5$ Hz), 7.96 (1H, d, $J = 7.5$ Hz), 7.85 (1H, d, $J = 9.3$ Hz), 7.57 (1H, d, $J = 7.5$ Hz), 7.53–7.52 (1H, m), 7.51–7.49 (1H, m), 7.43–7.41 (4H, m), 6.91 (1H, d, $J = 8.3$ Hz), 3.49 (3H, s). ¹³C NMR (400 MHz, CDCl₃): δ [ppm] = 154.30, 153.50, 141.13, 139.65, 137.90, 132.26, 129.50, 128.35, 127.44, 126.15, 125.22, 125.01, 122.92, 118.27, 115.77, 106.25, 105.17, 32.04. HRMS (ESI) calcd. for [C₂₀H₁₅N₂BF₂ + Na]⁺: 355.11921; found: 355.11884.

2.2.5. Synthesis of compound **2b**

Synthesis of the compound **2b** is according to the method of synthesis of compound **2a**.

Yield: 30.9%. ^1H NMR (300 MHz, CDCl_3): δ [ppm] = 8.10 (1H, d, $J = 9.3$ Hz), 8.00 (1H, d, $J = 7.2$ Hz), 7.95 (1H, d, $J = 7.8$ Hz), 7.84 (1H, d, $J = 7.2$ Hz), 7.55 (1H, t, $J = 7.8$ Hz), 7.40 (1H, d, $J = 9.3$ Hz), 7.32 (2H, d, $J = 9.0$ Hz), 7.04 (2H, d, $J = 9.0$ Hz), 6.95 (1H, d, $J = 9.6$ Hz), 3.88 (3H, s), 3.48 (3H, s). ^{13}C NMR (400 MHz, CDCl_3): δ [ppm] = 158.78, 154.14, 153.83, 139.51, 137.86, 133.82, 132.19, 132.17, 129.22, 126.09, 125.18, 124.94, 122.85, 118.23, 115.69, 114.76, 105.07, 55.54, 32.03. HRMS (ESI) calcd. for $[\text{C}_{21}\text{H}_{17}\text{ON}_2\text{BF}_2 + \text{Na}]^+$: 385.12979; found: 385.12949.

2.2.6. Synthesis of compound 2c

Synthesis of compound **2c** is according to the method of synthesis of compound **2a**.

Yield: 27.5%. ^1H NMR (300 MHz, CDCl_3): δ [ppm] = 8.15 (1H, d, $J = 9.6$ Hz), 8.03 (2H, dd, $J = 7.8$ Hz), 7.93 (1H, d, $J = 9.3$ Hz), 7.81 (2H, d, $J = 8.4$ Hz), 7.62 (1H, t, $J = 7.8$ Hz), 7.56 (2H, d, $J = 8.4$ Hz), 7.42 (1H, d, $J = 9.6$ Hz), 6.89 (1H, d, $J = 9.3$ Hz), 3.49 (3H, s). ^{13}C NMR (400 MHz, CDCl_3): δ [ppm] = 154.92, 152.56, 146.50, 145.81, 140.46, 138.43, 133.52, 132.89, 132.80, 129.44, 126.06, 125.36, 125.16, 123.46, 118.58, 117.61, 115.89, 111.14, 32.17. HRMS (ESI) calcd. for $[\text{C}_{21}\text{H}_{14}\text{N}_3\text{BF}_2 + \text{Na}]^+$: 380.11448; found: 380.11563.

2.2.7. Synthesis of compound 3a

The method to synthesize compound **3a** is similar with that of **2a**. Yield: 80.7%. ^1H NMR (300 M, CDCl_3): δ [ppm] = 8.36 (1H, d, $J = 4.4$ Hz), 8.35 (1H, d, $J = 3.2$ Hz), 8.23 (1H, d, $J = 1.6$ Hz), 8.00 (1H, d, $J = 9.6$ Hz), 7.75–7.73 (2H, m), 7.56–7.52 (3H, m), 7.45 (1H, t, $J = 7.2$ Hz), 7.37 (2H, d, $J = 8.8$ Hz), 7.05 (2H, d, $J = 2.0$ Hz), 6.97 (1H, d, $J = 9.6$ Hz), 3.89 (3H, s). ^{13}C NMR (400 MHz, CDCl_3): δ [ppm] = 165.39, 159.37, 158.60, 142.64, 140.57, 139.51, 138.17, 132.33, 132.23, 132.08, 129.22, 128.06, 127.34, 126.56, 126.12, 124.67, 122.60, 122.58, 118.59, 114.93, 55.59. HRMS (ESI) calcd. for $[\text{C}_{26}\text{H}_{18}\text{O}_2\text{NBF}_2 + \text{Na}]^+$: 448.12954; found: 448.12913.

2.2.8. Synthesis of compound 3b

The method to synthesize compound **3b** is similar with that of **3a**. Yield: 63.6%. ^1H NMR (300 M, CDCl_3): δ [ppm] = 8.47 (1H, d, $J = 1.6$), 8.39–8.34 (2H, m), 8.19 (1H, s), 8.02 (2H, d, $J = 9.6$ Hz), 7.97–7.85 (3H, m), 7.60–7.53 (3H, m), 7.37 (2H, d, $J = 7.8$ Hz), 7.05 (2H, d, $J = 7.8$ Hz), 6.98 (1H, d, $J = 9.6$ Hz), 3.88 (3H, s). ^{13}C NMR (400 MHz, CDCl_3): δ [ppm] = 165.43, 159.38, 158.63, 142.64, 140.58, 138.06, 136.77, 133.71, 132.87, 132.40, 132.32, 132.30, 129.04, 128.24, 128.08, 127.78, 126.77, 126.64, 126.52, 126.30, 126.21, 125.24, 124.73, 122.68, 122.65, 118.66, 114.94, 55.59. HRMS (ESI) calcd. for $[\text{C}_{30}\text{H}_{20}\text{O}_2\text{NBF}_2 + \text{Na}]^+$: 498.14526; found: 498.14553.

2.2.9. Synthesis of compound 3c

The method to synthesize compound **3c** is similar with that of **3a**. Yield: 89.6%. ^1H NMR (300 M, CDCl_3): δ [ppm] = 8.33 (1H, d, $J = 9.2$ Hz), 8.30 (1H, d, $J = 1.6$ Hz), 8.18 (1H, d, $J = 1.6$ Hz), 7.97 (1H, d, $J = 9.6$ Hz), 7.67 (2H, d, $J = 6.8$ Hz), 7.52 (1H, d, $J = 9.2$ Hz), 7.36 (2H, d, $J = 9.2$ Hz), 7.08–7.03 (4H, m), 6.95 (1H, d, $J = 9.6$ Hz), 3.90 (3H, s), 3.88 (3H, s). ^{13}C NMR (400 MHz, CDCl_3): δ [ppm] = 165.19, 159.75, 159.33, 158.55, 142.65, 140.49, 137.82, 132.35, 131.93, 131.90, 131.53, 128.39, 128.07, 126.56, 126.06, 124.26, 122.46, 118.46, 114.91, 114.65, 107.87, 55.58, 55.45. HRMS (ESI) calcd. for $[\text{C}_{27}\text{H}_{20}\text{O}_3\text{NBF}_2 + \text{Na}]^+$: 478.14012; found: 478.13972.

2.2.10. Synthesis of compound 3d

The method to synthesize compound **3d** is similar with that of **3a**. Yield: 26.2%. ^1H NMR (300 M, CDCl_3): δ [ppm] = 8.36 (2H, d, $J = 8.8$ Hz), 8.20 (1H, d, $J = 1.6$ Hz), 8.00 (1H, d, $J = 9.6$ Hz), 7.84 (4H, d, $J = 8.8$ Hz), 7.57 (1H, d, $J = 9.6$ Hz), 7.36 (2H, d, $J = 8.8$ Hz), 7.05 (2H, d, $J = 6.8$ Hz), 7.01 (1H, d, $J = 9.6$ Hz), 3.89 (3H, s). ^{13}C NMR (400 MHz, CDCl_3): δ [ppm] = 165.72, 159.47, 158.57, 143.97, 142.37,

140.51, 135.89, 132.97, 132.11, 132.01, 130.44, 127.96, 126.54, 126.33, 125.34, 123.04, 119.10, 118.02, 114.96, 111.75, 107.82, 55.59. HRMS (ESI) calcd. for $[\text{C}_{27}\text{H}_{17}\text{O}_2\text{N}_2\text{BF}_2 + \text{Na}]^+$: 473.12481; found: 473.12578.

2.2.11. Synthesis of compound 4a

The method to synthesize compound **4a** is similar with that of **1a**. Through displacing fluorine by a phenyl group in the compound **3a** (obtained above), the compound **4a** was obtained as a solid. Yield: 50.3%. ^1H NMR (400 M, CDCl_3): δ [ppm] = 8.11 (1H, d, $J = 1.2$ Hz), 8.06 (1H, d, $J = 9.2$ Hz), 8.00 (1H, d, $J = 1.2$ Hz), 7.73 (1H, d, $J = 10.0$ Hz), 7.69 (2H, d, $J = 7.2$ Hz), 7.52–7.41 (7H, m), 7.26 (1H, d, $J = 10.0$ Hz), 7.19–7.13 (6H, m), 6.86 (2H, d, $J = 9.2$ Hz), 6.78 (1H, d, $J = 9.6$ Hz), 6.69 (2H, d, $J = 8.8$ Hz), 3.74 (3H, s). ^{13}C NMR (400 MHz, CDCl_3): δ [ppm] = 168.06, 158.75, 158.21, 141.08, 139.85, 137.06, 135.72, 133.79, 131.40, 131.22, 129.11, 128.50, 127.76, 126.26, 126.15, 126.07, 125.98, 123.64, 120.11, 114.06, 109.78, 55.40. HRMS (ESI) calcd. for $[\text{C}_{38}\text{H}_{28}\text{BNO}_2 + \text{H}]^+$: 542.22923; found: 542.23000.

2.2.12. Synthesis of compound 4b

The method to synthesize compound **4b** is similar with that of **4a**. Yield: 42.6%. ^1H NMR (300 M, CDCl_3): δ [ppm] = 8.23 (1H, s), 8.12 (2H, m), 8.08 (1H, d, $J = 9.0$ Hz), 8.00–7.88 (3H, m), 7.82 (1H, d, $J = 8.4$ Hz), 7.76 (1H, d, $J = 9.6$ Hz), 7.55–7.47 (6H, m), 7.28 (1H, d, $J = 9.0$ Hz), 7.20–7.13 (6H, m), 6.86 (2H, d, $J = 9.0$ Hz), 6.78 (1H, d, $J = 9.6$ Hz), 6.69 (2H, d, $J = 9.0$ Hz), 3.74 (3H, s). ^{13}C NMR (400 MHz, CDCl_3): δ [ppm] = 168.07, 158.73, 158.20, 141.06, 139.84, 137.08, 136.89, 135.68, 133.76, 133.70, 132.73, 131.58, 131.35, 128.84, 128.48, 128.17, 127.72, 126.73, 126.62, 126.31, 126.28, 126.22, 126.05, 126.02, 125.87, 125.21, 123.68, 120.13, 114.03, 109.77, 55.33. HRMS (ESI) calcd. for $[\text{C}_{42}\text{H}_{30}\text{BNO}_2 + \text{H}]^+$: 592.24454; found: 592.24450.

2.2.13. Synthesis of compound 4c

The method to synthesize compound **4c** is similar with that of **4a**. Yield: 51.6%. ^1H NMR (300 M, CDCl_3): δ [ppm] = 8.04 (2H, d, $J = 9.0$ Hz), 7.96 (1H, d, $J = 3.0$ Hz), 7.72 (1H, d, $J = 9.6$ Hz), 7.62 (2H, d, $J = 8.7$ Hz), 7.48–7.45 (4H, m), 7.26 (1H, d, $J = 9.0$ Hz), 7.19–7.12 (6H, m), 7.03 (2H, d, $J = 8.7$ Hz), 6.86 (2H, d, $J = 9.0$ Hz), 6.77 (1H, d, $J = 9.6$ Hz), 6.68 (2H, d, $J = 9.0$ Hz), 3.88 (3H, s), 3.74 (3H, s). ^{13}C NMR (400 MHz, CDCl_3): δ [ppm] = 167.91, 159.52, 158.73, 158.19, 141.10, 139.79, 136.76, 135.78, 133.80, 132.32, 130.96, 130.90, 128.52, 126.75, 126.30, 126.13, 126.05, 125.86, 125.62, 123.56, 120.03, 114.55, 114.05, 109.81, 55.46, 55.36. HRMS (ESI) calcd. for $[\text{C}_{39}\text{H}_{30}\text{BNO}_3 + \text{H}]^+$: 572.23981; found: 572.23995.

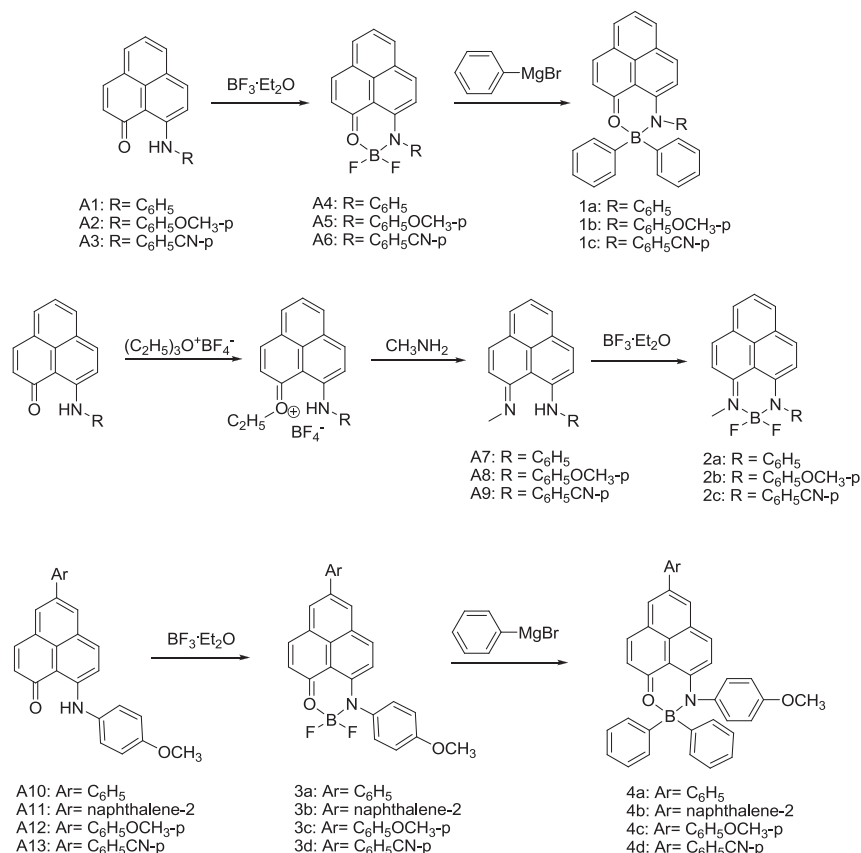
2.2.14. Synthesis of compound 4d

The method to synthesize compound **4d** is similar with that of **4a**. Yield: 33.7%. ^1H NMR (400 M, CDCl_3): δ [ppm] = 8.11 (1H, d, $J = 1.6$ Hz), 8.08 (1H, d, $J = 9.2$ Hz), 7.98 (1H, d, $J = 1.6$ Hz), 7.80 (4H, m), 7.73 (1H, d, $J = 10.0$ Hz), 7.48–7.45 (4H, m), 7.29 (1H, d, $J = 9.2$ Hz), 7.20–7.14 (6H, m), 6.85 (2H, d, $J = 9.2$ Hz), 6.81 (1H, d, $J = 9.6$ Hz), 6.70 (2H, d, $J = 9.2$ Hz), 3.74 (3H, s). ^{13}C NMR (400 MHz, CDCl_3): δ [ppm] = 167.48, 157.70, 157.35, 143.36, 139.79, 139.70, 138.72, 134.48, 133.79, 133.14, 132.70, 131.86, 130.31, 129.81, 129.53, 127.84, 127.52, 127.41, 126.69, 125.93, 125.27, 125.12, 124.46, 123.18, 54.34. HRMS (ESI) calcd. for $[\text{C}_{39}\text{H}_{27}\text{BN}_2\text{O}_2 + \text{H}]^+$: 567.22450; found: 567.22532.

3. Results and discussion

3.1. Synthesis

The synthetic routes and chemical structures of the compounds **1(a,b,c)**, **2(a,b,c)**, **3(a,b,c,d)** and **4(a,b,c,d)** are depicted in Scheme 1.



Scheme 1. Synthesis of phenalenyl-based phenyl-boron complex-type compound **1(a,b,c)**, **2(a,b,c)**, **3(a,b,c,d)** and **4(a,b,c,d)**.

Briefly, these compounds are constructed by a large rigid planar π -system with different sterical hindered substituents on the tip of the phenalene plane, on the nitrogen atom or boron atom. Compounds **A1–A13** were synthesized using a methodology previously described [8,9]. The fluorophores **2a–2c** and **3a–3d** were synthesized in 30–80% yields by treatment **A7–A13** with BF₃ in *o*-xylene. Diphenyl-boron-coordinated compounds **1a–1c** and **4a–4d** were obtained by substituting the fluorine using a phenylMgBr Grignard reagent. The reaction proceeded with moderate yield between 30% and 50% at room temperature under argon.

3.2. Crystal structure analysis

These boron-based compounds are soluble in common organic solvents such as THF and CH₂Cl₂ but insoluble in water. The crystals of **1b**, **2b** and **4a** were grown from CH₂Cl₂/hexane solution and analyzed by single-crystal X-ray diffraction. The ORTEP plots are depicted in Fig. 2, from which we can see that the substituents on boron were not coplanar with the rigid plane, and the aryl-substitute on nitrogen induced twisted conformations. The molecular packing of **1b**, **2b** and **4a** in the crystalline state are shown in Fig. 3.

It can be seen that the compound **2b** are located in a face-to-face pattern, but not parallel. As shown in crystal **1b** and **4a**, the phenalene core plane of the neighboring molecules are not a vertical-alignment. They contain bulky substituents on nitrogen and boron which inhibit the close stacking of the phenalene rigid plane and weak the strong π – π stacking effect of the phenalene plane which is favorable for fluorescent emission. Combining the crystal data of the **DFBPLY**, it was concluded that the bulky substitute on nitrogen atom is the necessary prerequisite for this kind of compounds to get

the aggregation-induced emission property. Because the packing of the molecules and the intermolecular distance mainly depend on the bulky substituents on nitrogen atom, not the substituents on the tip carbon atom of phenalene plane or fluorine/phenyl groups on the boron atom.

The theoretical calculations carried out by the B3LYP/6-31G* basis set, reveal that for each compound, aryl-substituents on the nitrogen atom and substituents on the boron atom form the conjugated orbital through and with the boron atom (Fig. 4). These aryl-substituents have significant contributions to HOMOs with electronic clouds located near the boron atom. For the compounds **1a–1c** and **4a–4d**, the HOMO orbitals are delocalized over the whole molecule; whilst a dense electronic cloud of the LUMO orbitals is mostly located on the phenalene rigid plane [10], as shown in Fig. 4 and Fig. S1. For **2a–2c**, the electronic cloud located on fluorine indicates a form of the intramolecular push–pull effect, which is favorable for fluorescent emission of the compounds [4b]. The DFT calculations indicate that phenalene-BF₂ derivatives **2a–2c**, **3a–3d**, shows intramolecular charge transfer transition from aryl groups on the tip carbon atom of phenalene plane and nitrogen atom to the BF₂ moiety, which may be the reason that compounds **2a–2c**, **3a–3d** show higher solid-emission intensity than that of compounds **1a–1c** and **4a–4d**.

3.3. Spectroscopic properties

The visible absorption and fluorescence spectroscopic data of **1a–4d** in solution and solid state are shown in Fig. 5, Fig. S2 and summarized in Table 1. In THF solution, compounds **1a**, **1b** and **1c** show similar absorption spectra with two absorbance regions. Their absorption maxima are at around 380 nm and 510 nm,

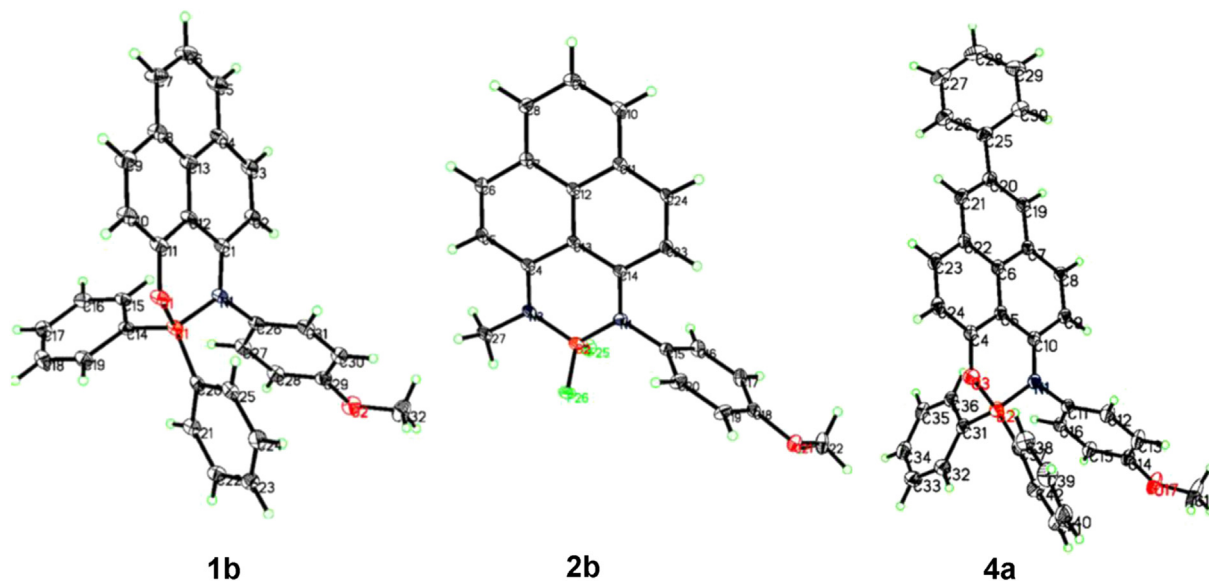


Fig. 2. ORTEP drawings of compounds **1b** (CCDC 965229), **2b** (CCDC 965230), and **4a** (CCDC 965231).

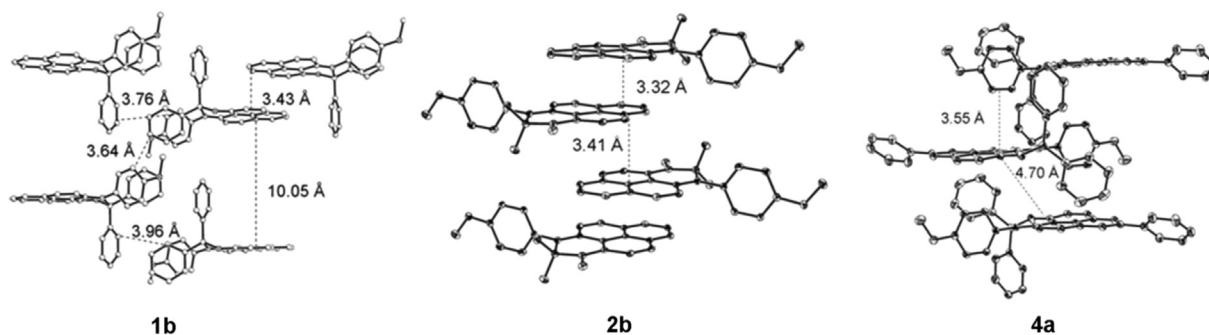


Fig. 3. Molecular packings of compounds **1b**, **2b** and **4a** in crystals, with indicated distance between the planes. Hydrogen atoms are omitted for clarity.

respectively, as shown by the black curve in Fig. 5A and Fig. S2A. There is a 10 nm and 60 nm red-shift compared with that of DFBPLY (370 nm, 450 nm) [8], due to conjugated effect of two-phenyl rings on boron atom. Compounds **2a–2c** show maxima absorption at around 370 nm and 490 nm, with 40 nm red-shift after using the NCH₃ group to substitute the oxygen atom (Fig. S2A). Compounds **3a–3d** show maxima absorption at around 370 nm and 480 nm, with 30 nm red-shift while directly

connecting the aryl group onto the tip carbon of phenalenyl ring (Fig. S2B).

In Fig. 5B, Fig. S2C and S2D and Table 1, absorption spectra of new compounds in solid state also show two absorption maxima similar to those in THF, but with about 20 nm red-shift for compounds **1a–1c** and with about 15 nm red-shift for **2a–2c** compared with that in THF; at the same time, there are almost 20 nm red-shift for compounds **3a–3d** and about 40 nm red-shift for compounds

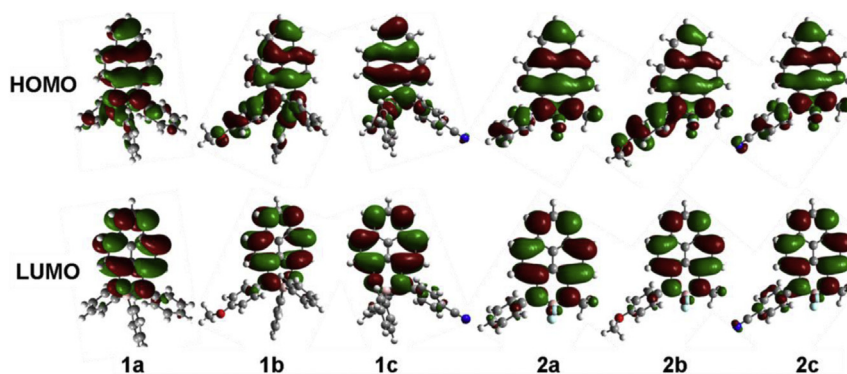


Fig. 4. Optimized molecular structures, and molecular orbital amplitude plots of HOMOs and LUMOs of compounds **1(a,b,c)** and **2(a,b,c)** calculated using B3LYP/6-31G*.

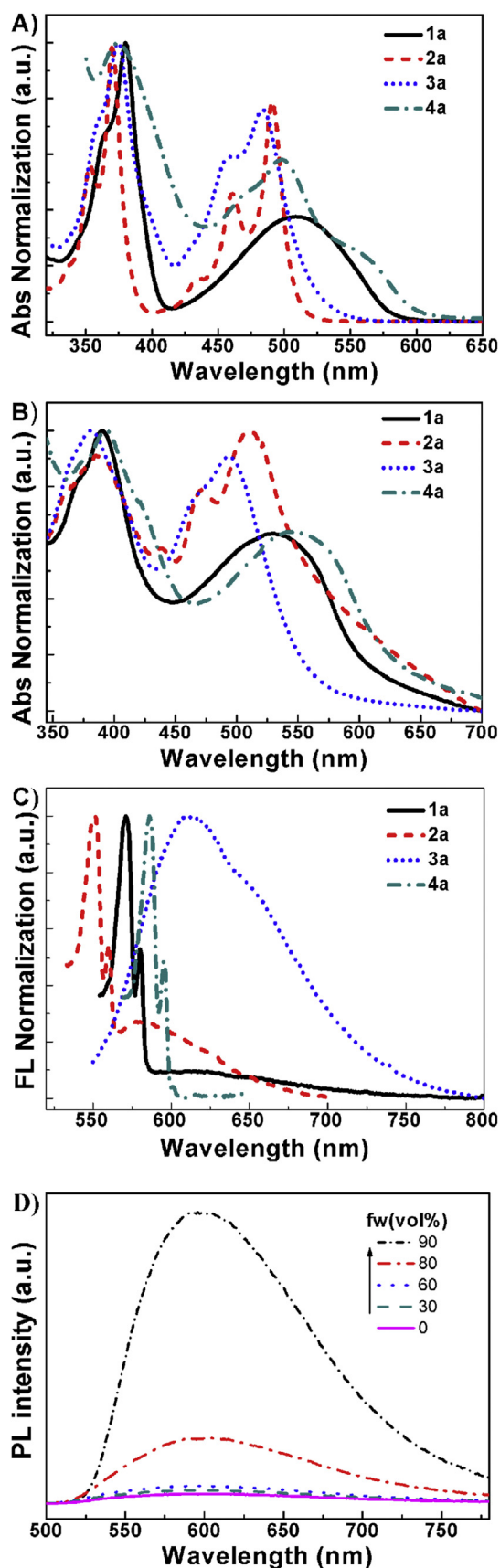


Fig. 5. (A) Absorption spectra of **1a**, **2a**, **3a** and **4a** in THF solutions. (B) Absorption spectra of **1a**, **2a**, **3a** and **4a** in solid film. (C) PL spectra of **1a**, **2a**, **3a** and **4a** in solid film, excited at maximum excitation wavelength. (D) PL spectra of **2b** in THF/water mixtures with different water fraction (fw), excited at 410 nm.

4a, **4c** and **4d** compared with that in THF. Moreover, it was noted that solid film absorption maxima of **1a–1c** is about 30 nm red-shift compared with solid film absorption of **DFBPLY** (about 500 nm).

Compounds **1a–4d** exhibit very weak emission in dilute THF solutions. The fluorescence quantum yields (Φ_F) in solutions are measured below 0.01 (Table S1). However, their fluorescence emissions in solid state are enhanced for ten times more than that in solution according to the quantum yield, which show the obvious aggregation-induced emission effect [5]. The emission maxima of the compounds **1a–1c** and **3a–3d** have 30 nm and 60 nm red-shift, respectively, compared with those of **DFBPLY** (about 550 nm) in Figs. 5C, 2E and F.

We also further investigated the AIE effect of these organoboron compounds by adding water into their THF solutions and recording the change of PL spectra in THF/water mixtures (illustrated in Fig. 5D using compound **2b** as an example). It can be seen that an emission band appears and is boosted drastically when a large amount of water (90% vol%) is added. Since water is a poor solvent for these compounds, the molecules are aggregated in aqueous solutions. As shown in Fig. S2, when up to 90% water is added to the THF solution, the spectral profile is greatly changed, and a new, clear shoulder peak appears at about 500 nm, due to the packing of the molecules, which is corresponding to the maximum absorption of **2b** at 507 nm in film. The abrupt change in the absorbance at 90% water fraction agrees well with the sudden jump in the intensity of the emission shown in Fig. 5D, confirming that the compound **2b** greatly aggregates in 90% aqueous solutions. It is believed that the intramolecular rotations in compounds **1a–4d** are inhibited and also the large block groups prevent the intermolecular approaching and interaction. So the energy loss of the non-radiative transition is reduced and the radiative transition is enhanced in the solid state.

Enhanced solid emissions are also shown from the solid powder and aggregated solution of compounds **1b** and **2b**. In Fig. 6A, compounds **1b** and **2b** emit very weak fluorescence in THF solution under 365 nm light. However, they exhibit strong yellow and orangepink light, respectively for compounds **1b** and **2b** in aggregation and solid state, as shown in Fig. 6B and C, again confirming their AIE characteristics.

The solid film of compounds **1a–4d** exhibit strong yellow light in the range of 550–620 nm (Table 1). The Φ_F values of these organoboron fluorophores **1a–4d** in film enhance more than 10

Table 1
Photoelectric physical properties of compound **1a–4d**.

Compound	$\lambda_{\text{abs}}^{\text{max}}$ (nm) Solution ^a ($\text{M}^{-1} \text{cm}^{-1}$)	$\lambda_{\text{em}}^{\text{max}}$ (nm) Film ^b	Φ_F (%) ^c Film (ev)	HOMO ^d (ev)	LUMO ^d (ev)	E_g^d (ev)
1a	509(40,600)	571	68	-5.14	-3.11	2.03
1b	516(30,000)	572	51	-5.49	-3.05	1.99
1c	517(61,400)	585	58	-5.12	-3.15	1.97
2a	491(19,600)	551	24	-5.28	-3.13	2.15
2b	492(22,400)	547	89	-5.40	-3.18	2.22
2c	491(13,100)	545	43	-5.29	-3.09	2.20
3a	484(55,200)	612	84	-5.26	-3.03	2.23
3b	488(55,300)	609	66	-5.26	-3.08	2.18
3c	492(52,000)	615	65	-5.29	-3.24	2.05
3d	479(57,700)	619	41	-5.24	-3.29	1.95
4a	499(33,600)	580	10	-5.23	-3.29	1.94
4b	531(74,800)	589	18	-5.22	-3.24	1.98
4c	493(39,000)	603	22	-5.31	-3.18	2.13
4d	489(73,000)	586	48	-5.33	-3.39	1.94

^a In THF solution (10 μm).

^b Film drop-casted on quartz plate.

^c Determined in amorphous film by integrating sphere.

^d HOMO (I_{Fc}) = -e (E_{ox}) + (-4.8) eV, $E_g = 1240/\lambda_g$, LUMO = HOMO - E_g .

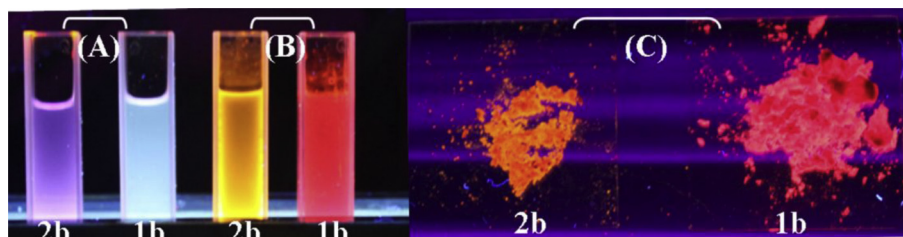


Fig. 6. Photos of (A) THF solution, (B) aqueous solution (Vol/THF:Vol/H₂O = 10:90), (C) powders of **1b** and **2b**, taken under the illumination of 365 nm UV light.

times than that in solution (Φ_F in THF <1%, shown in Supporting information), due to the AIE effect.

As shown in Table 1, for compounds **1a–1c**, through substituting fluorine using an aryl group on the boron atom (coordination center), compared with model compound **DFBPLY**: it can be seen that: 1) the solid emissive intensity is enhanced due to the aryl steric effect; and 2) wavelengths are red-shifted due to conjugated effect in the aggregation state. Also, similar results are obtained for compounds **2a–2c** while changing the coordinated oxygen atom into an $-NCH_3$ group or adding an aryl conjugated group onto tip-carbon of the phenalene plane for compounds **3a–3d**.

Compared with compounds **3a–3d**, surprisingly, the solid emissive intensity of compounds **4a–4c** weakened except for **4d**, maybe due to the electronic-pull property of the $-PhCN$ substitute in compound **4d**. Meanwhile emissive wavelength compounds **4a–4c** are all blue-shifted compared with **3a–3d**, in spite of long intermolecular distance as shown in crystal packing of compound **4a** in Fig. 3. One deduced possible reason for this is that after substituting the fluorine by phenyl, the intramolecular charge transfer property is greatly weakened, which is not benign for fluorescent emission [4b,11].

4. Conclusions

In conclusion, a novel series of four-coordinate boron complex-type fluorophores, with enhanced fluorescence emission in the solid state, have been synthesized. We systematically studied the effect of introducing electron-donating or electron-withdrawing substituent groups onto the tip-carbon atom of the phenalene plane of compounds, onto the nitrogen atom or boron atom. The X-ray structure demonstrated that the bulky substitute on nitrogen atom is the necessary prerequisite for this kind of compounds to get the intensive aggregation-induced emission, which could effectively prevent the fluorophores forming short intermolecular interactions. Through changing the substituent groups, the emission in the solid-state of these compounds could change from green to yellow to red. Phenalene- BF_2 derivatives **2a–2c**, **3a–3d** shows higher Φ_F values compared with that of **1a–1c** and **4a–4c** except **4d**, maybe due to the intramolecular donor–acceptor electronic features between phenalene plane or nitrogen atom and the BF_2 moiety.

To obtain strong solid emissive fluorescent compounds, it was found that structures should feature big block substituents to create large distances between molecules. This then lowered the intermolecular effect and reduced non-radiative energy loss. Moreover, another determinant was found to be intramolecular electronic properties such as intramolecular donor–acceptor electronic features with a tendency to form intramolecular charge transfer. This can further induce intense solid fluorescent emission.

Acknowledgments

The authors gratefully acknowledge the financial support from the National Basic Research Program (2011CB933303) and the National Natural Science Foundation of China (NSFC) (21321001, 21371012).

Appendix A. Supplementary data

Supplementary data related to this article can be found at <http://dx.doi.org/10.1016/j.dyepig.2014.03.017>.

References

- (a) De Silva AP, Gunaratne HQN, Gunnlaugsson T, Huxley AJM, McCoy CP, Rademacher JT, et al. Signaling recognition events with fluorescent sensors and switches. *Chem Rev* 1997;97(5):1515–66;
(b) Wang M, Zhang DQ, Zhang GX, Zhu DB. The convenient fluorescence turn-on detection of heparin with a silole derivative featuring an ammonium group. *Chem Commun*; 2008:4469–71.
- (a) Yang W, He H, Drueckhammer DG. Computer-guided design in molecular recognition: design and synthesis of a glucopyranose receptor. *Angew Chem Int Ed Engl* 2001;40(9):1714–8;
(b) Hong YN, Häußler M, Lam JWY, Li Z, Sin KK, Dong YQ, et al. Label-free fluorescent probing of G-quadruplex formation and real-time monitoring of DNA folding by a quaternized tetraphenylethene salt with aggregation-induced emission characteristics. *Chemistry – Eur J* 2008;14(21):6428–37;
(c) Wang M, Zhang DQ, Zhang GX, Tang YL, Wang S, Zhu DB. Fluorescence turn-on detection of DNA and label-free fluorescence nuclease assay based on the aggregation-induced emission of silole. *Anal Chem* 2008;80(16):6443–8.
- (a) Liu QD, Mudadu MS, Thummel R, Tao Y, Wang SN. From blue to red: syntheses, structures, electronic and electroluminescent properties of tunable luminescent N, N chelate boron complexes. *Adv Funct Mater* 2005;15(1):143–54;
(b) Chen CT. Evolution of red organic light-emitting diodes: materials and devices. *Chem Mater* 2004;16(23):4389–400.
- (a) Hepp A, Uirich G, Schmechel R, von Seggern H, Ziessel R. Highly efficient energy transfer to a novel organic dye in OLED devices. *Synth Met* 2004;46(1):11–5;
(b) Zhou Y, Chi S, Qian XH. Isomeric boron-fluorine complexes with donor-acceptor architecture: strong solid/liquid fluorescence and large Stokes shift. *Org Lett* 2008;10(4):633–6.
- (a) Luo JD, Xue ZL, Jacky W, Lam Y, Cheng L, Chen HY, et al. Aggregation-induced emission of 1-methyl-1,2,3,4,5-pentaphenylsilole. *Chem Commun*; 2001:1740–1;
(b) Yu G, Yin SW, Liu YQ, Chen JS, Xu XJ, Sun XB, et al. Structures, electronic states, photoluminescence, and carrier transport properties of 1,1-disubstituted 2,3,4,5-tetraphenylsiloles. *J Am Chem Soc* 2005;127(17):6335–46;
(c) Li Z, Dong YQ, Lam JWY, Sun J, Qin A, Häußler M, et al. Functionalized siloles: versatile synthesis, aggregation-induced emission, and sensory and device application. *Adv Funct Mater* 2009;19(6):905–17;
(d) Zhao Z, Chen S, Chan CYK, Lam JWY, Jim CKW, Lu P, et al. A facile and versatile approach to efficient luminescent materials for applications in organic light-emitting diodes. *Chemistry – Asian J* 2012;7(3):484–8.
- (a) Chen HY, Lam WY, Luo JD, Ho YL, Tang BZ, Zhu DB, et al. Highly efficient organic light-emitting diodes with a silole-based compound. *Appl Phys Lett* 2002;81(4):574–6;
(b) Dong YQ, Jacky WY, Lam AJQ, Liu JZ, Li Z, Tang BZ, et al. Aggregation-induced emissions of tetraphenylethene derivatives and their utilities as chemical vapor sensors and in organic light-emitting diodes. *Appl Phys Lett* 2007;91(1):011111–3.
- (a) Wakamiya A, Mishima K, Ekawa K, Yamaguchi S. Kinetically stabilized dibenzoborole as an electron-accepting building unit. *Chem Commun*; 2008:579–81;

- (b) Zhao CH, Wakamiya A, Inukai Y, Yamaguchi S. Highly emissive organic solids containing 2,5-diboryl-1,4-phenylene unit. *J Am Chem Soc* 2006;128(50):15934–5.
- [8] (c) Entwistle CD, Marder TB. Boron chemistry lights the way: optical properties of molecular and polymeric systems. *Angew Chem Int Ed Engl* 2002;41(16):2927–31.
- [8] Yan WB, Wan XJ, Chen YS. Phenalenyl-based boron-fluorine complexes: synthesis, crystal structures and solid-state fluorescence properties. *J Mol Struct* 2010;968(1–3):85–8.
- [9] Yan WB, Wan XJ, Xu YF, Lv X, Chen YS. A phenalenyl-based neutral stable π -conjugated polyradical. *Synth Met* 2009;159(17–18):1772–7.
- [10] Zhou J, He BR, Bin Chen, Ping Lu, Sung HHY, Williams ID, et al. Deep blue fluorescent 2,5-bis(phenylsilyl)-substituted 3,4-diphenylsiloles: synthesis, structure and aggregation-induced emission. *Dye Pigments* 2013;99(2):520–5.
- [11] Hu R, Lager E, Aguilar AA, Liu JZ, Lam JWY, Sung HHY, et al. Twisted intramolecular charge transfer and aggregation-induced emission of BODIPY derivatives. *J Phys Chem C* 2009;113(36):15845–53.